

Magnetotransport properties of strained $\text{Ga}_{0.95}\text{Mn}_{0.05}\text{As}$ epilayers close to the metal-insulator transition: Description using Aronov-Altshuler three-dimensional scaling theory

J. Honolka,^{1,2,*} S. Masmanidis,² H. X. Tang,² D. D. Awschalom,³ and M. L. Roukes²

¹Max-Planck-Institut für Festkörperforschung, Heisenbergstrasse 1, 70569 Stuttgart, Germany

²Condensed Matter Physics 114-36, California Institute of Technology, Pasadena, California 91125, USA

³Department of Physics, University of California, Santa Barbara, California 93106, USA

(Received 7 March 2007; revised manuscript received 11 April 2007; published 7 June 2007)

The magnitude of the anisotropic magnetoresistance (AMR) and the longitudinal resistance in compressively strained $\text{Ga}_{0.95}\text{Mn}_{0.05}\text{As}$ epilayers were measured down to temperatures as low as 30 mK. Below temperatures of 3 K, the conductivity decreases $\propto T^{1/3}$ over 2 orders of magnitude in temperature. The conductivity can be well described within the framework of a three-dimensional scaling theory of Anderson's transition in the presence of spin scattering in semiconductors. It is shown that the samples are on the metallic side but very close to the metal-insulator transition. At lowest temperatures, a decrease in the AMR effect is observed, which is assigned to changes in the coupling between the remaining itinerant carriers and the local Mn 5/2-spin moments.

DOI: [10.1103/PhysRevB.75.245310](https://doi.org/10.1103/PhysRevB.75.245310)

PACS number(s): 85.75.-d, 71.30.+h, 72.20.My, 75.47.-m

INTRODUCTION

Mn-doped diluted III-V semiconductors have been of great interest since the discovery of a ferromagnetic phase at low temperatures.¹ The prospect of using diluted ferromagnets as spin injectors in spintronic devices has initiated multiple research efforts to understand their fundamental magnetic properties and to control important parameters such as the magnetic anisotropy energy or the Curie temperature.²⁻⁴ Though several mechanisms have been proposed to theoretically describe ferromagnetism in dilute magnetic semiconductors (DMSs), a profound understanding is still elusive. It is widely accepted though that in the case of GaMnAs, holes in the valence band produced by the Mn dopants play the key role in mediating the interaction between spin 5/2 Mn sites. However, since ferromagnetism was found in both the metallic and insulating phases of DMSs, the correlation between magnetism and transport is expected to be rather complex. In the metallic regime, ferromagnetic coupling between the local Mn spins via spin polarization of *p*-type carriers is often described by Zener type mean-field models.^{5,6} Approaching the metal-insulator transition (MIT) localization effects due to disorder becomes increasingly important, which alters the magnetic behavior as described by models taking into account spatial inhomogeneities.⁷⁻¹⁰

Experimentally, the combined study of conductivity and magnetotransport is a powerful tool to characterize DMSs in the viewpoint of carrier localization and magnetic properties. Most magnetotransport studies, so far, were done on the anomalous Hall effect in the high magnetic field regime using classic Hall-bar geometries with applied fields perpendicular to the current. A complementary approach to gain information on the magnetic properties is the study of the anisotropic magnetoresistance effect. The latter was shown to induce rather large Hall-resistance jumps up to 80 Ω during reorientation of the magnetization in ferromagnetic GaMnAs epilayers.¹¹ In this work, we present a study of the conductivity and the anisotropic magnetoresistance (AMR) behavior of $\text{Ga}_{0.95}\text{Mn}_{0.05}\text{As}$ epilayers down to temperatures

as low as 30 mK. We show that in the lowest temperature regime, the transport can be well described by the three-dimensional (3D) scaling theory of Anderson's transition. Our results thus offer an alternative interpretation to very recent reports on the low temperature conductivity of metallic GaMn(5%)As epilayers, where weak localization¹² and Kondo models¹³ are employed. A small reduction of the AMR signal toward lowest temperatures will be discussed in terms of a localization dependent ferromagnetic coupling between Mn spins.

EXPERIMENT

We studied $\text{Ga}_{0.95}\text{Mn}_{0.05}\text{As}$ epilayers of 150 nm thickness grown on a insulating GaAs(001) substrate with a buffer layer fabricated by means of molecular beam epitaxy at 250 °C. Because of the compressive strain in the film introduced by the lattice mismatch with the substrate, the material is known to have a magnetic easy axis in the plane¹⁴ with a Curie temperature of $T_c \approx 45$ K in the case of our samples. The epilayer is patterned into a 100 μm wide Hall bar oriented along the [110] direction using electron beam lithography. Multiple voltage probes 100 μm apart at both sides of the bar are used to measure the Hall resistance and the longitudinal resistance per square (see sketch in Fig. 1). Further experimental details are given elsewhere.¹¹ In-plane magnetic fields up to $H=2$ kOe were generated by a superconducting Nb coil. Field dependent measurements were therefore limited to the temperature range below the critical temperature of the superconducting coil of about 5 K. The angle ϕ_H between the field orientation and the [110] direction within the plane of the epilayer was set to 15° as indicated in Fig. 1. Special care was taken to ensure sufficient thermal coupling between the sample and the cold finger of the dilution refrigerator. To minimize external rf heating, the entire setup is placed inside a shielded room and, additionally, leads to the sample are RC filtered with a cutoff frequency of a few kilohertz. For every temperature, the amplitude of the bias current was chosen to optimize the signal to

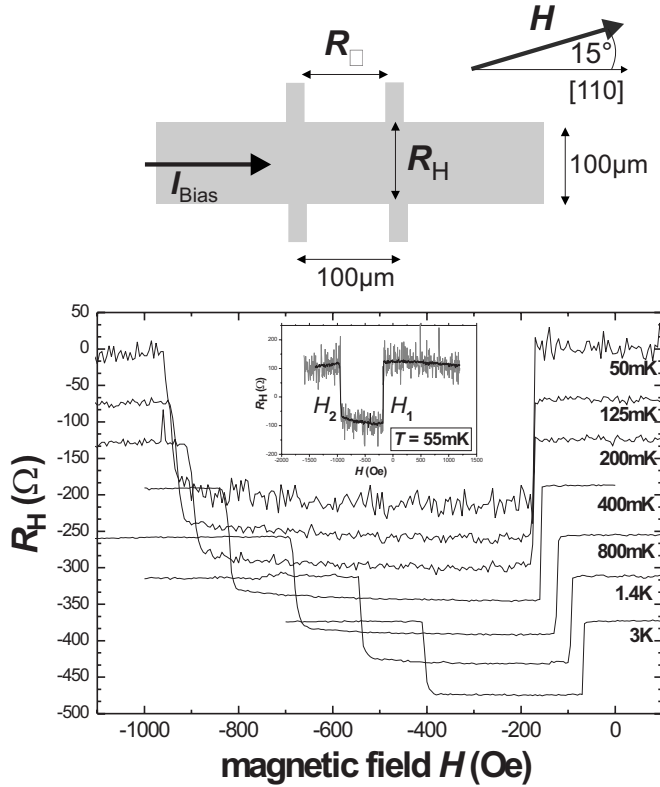


FIG. 1. Hall-resistance measurements while ramping the in-plane magnetic field at an average speed of 0.4 Oe/s for different temperatures. The curves are shifted by a constant offset with respect to each other. The increased noise at low temperatures is due to the reduction of the bias current. In the inset, two measurements for bias currents of 100 pA (gray) and 1 nA (black) at $T=55$ mK are shown for comparison.

noise ratio without heating the sample. At lowest temperatures, the currents had to be reduced to 500 pA, while above 1 K, current amplitudes of 10 nA could be used. Measurements while sweeping the magnetic field have been obtained in steps of 5 Oe with an average ramping speed of 0.4 Oe/s. These low ramping speeds were necessary at lowest temperatures to avoid heating effects due to eddy currents.

RESULTS

According to AMR theory, both the measured longitudinal resistance and the Hall resistance depend on the orientation of the magnetization with respect to the bias current direction. For the case of a single domain magnetized $100 \times 100 \mu\text{m}^2$ square, this can be expressed as

$$R_{\square} = [\rho_{\parallel} + (\rho_{\parallel} - \rho_{\perp}) \cos^2 \phi] / t, \quad (1)$$

$$R_H = (\rho_{\parallel} - \rho_{\perp}) \sin \phi \cos \phi / t, \quad (2)$$

where R_{\square} and R_H are the longitudinal and the Hall resistance per square, respectively. ϕ is the angle between the magnetization M and the bias current, $\rho_{\parallel}(\rho_{\perp})$ the resistivity for currents parallel (perpendicular) to the magnetization, and t the thickness of the epilayer. We want to comment at this

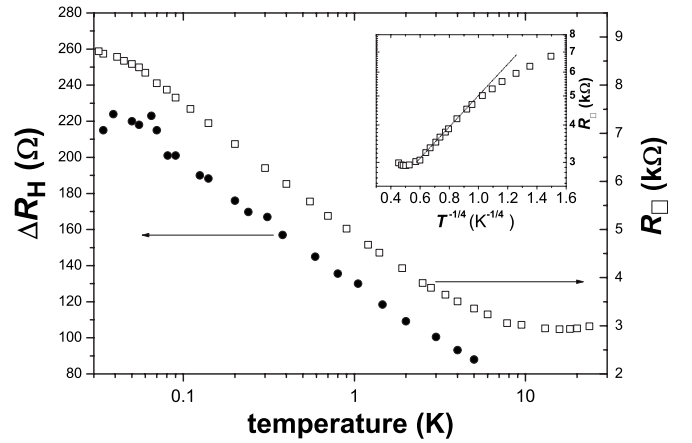


FIG. 2. (\square) Temperature dependence of the longitudinal resistance per square measured at a bias current of 1 nA and zero magnetic field. Prior to the measurement, the sample was magnetized at $H_S=2$ kOe. (\bullet) Temperature dependence of the first Hall-resistance jump (H_1) evaluated at the maximum and minimum values of $R_H(H)$.

point that AMR theories were originally developed to describe ferromagnetic metals, which will not be applicable on diluted magnetic semiconductors without modification. For the case of transition metals with strong exchange splitting of the d bands, $(\rho_{\parallel} - \rho_{\perp})$ is a positive value and is believed to result from anisotropic sd scattering of minority spin electrons into extended d -band states. In GaMnAs, however, the spin dependent scattering channels of the p -type hole carriers with, e.g., single localized Mn spins are different and more complex. This is reflected in the fact that $(\rho_{\parallel} - \rho_{\perp})$ is experimentally found to be negative in compressively strained GaMnAs with Mn concentrations around 5%–8%, which was recently explained theoretically.¹⁵

In Fig. 1, the Hall resistance $R_H(H)$ is shown for selected temperatures, while the in-plane magnetic field is ramped from positive to negative values. The two jump behavior of the curves in Fig. 1 can be modeled if one assumes a free energy density of the form $E = K_u \sin^2 \phi + (K_1/4) \cos^2(2\phi) - MH \sin(\phi - \phi_H)$ as described elsewhere,¹¹ leading to four local minima at $\phi_{1,2} = \pm(\pi/4 - \delta)$ and $\phi_{3,4} = \pm(3\pi/4 + \delta)$ for $H=0$. Here, K_u and K_1 are the in-plane uniaxial and cubic anisotropy constants and $\delta = \sin^{-1}(K_u/K_1)$. The two jumps observed in the data in Fig. 1 then reflect the sequential transitions of the magnetization orientation from $[100]$ ($\phi \sim -45^\circ$) via $[010]$ ($\phi \sim +45^\circ$) to $[100]$ ($\phi \sim +135^\circ$). During each transition, a single 90° domain wall travels through the sample. The magnitude of the observed jumps in R_H increases with decreasing temperature and at the same time H_1 and H_2 are both shifted to larger absolute values. For the evaluation of the magnitude of the AMR, we chose the transition at H_1 since it is more abrupt and therefore better defined compared to that at H_2 , which seems to happen more gradually. In order to exclude Stoner rotation effects, the magnitude of the first jump, ΔR_H , was evaluated at the maximum and minimum values of $R_H(H)$, which correspond to well defined values of $\phi = \pm(\pi/4)$. As shown in Fig. 2, ΔR_H is increasing with decreasing temperature and a maximum

value of 220Ω is reached at around 40–50 mK. Again, we want to emphasize that it was assured that decreasing the magnetic field ramping speed or bias current did not alter the results of the Hall-resistance measurements even at lowest temperatures (see inset of Fig. 1).

For comparison, the measured longitudinal resistance R_{\square} at static field conditions $H=0$ is shown in Fig. 2. Prior to the resistance measurement the sample was uniformly magnetized using a saturating field $H_S=2$ kOe. At about 16 ± 2 K, a minimum in the resistance appears, which is consistent with earlier measurements.^{11,16} At lower temperatures, the resistance rises monotonously and in the range between 1.5 K and 50 mK seems to follow the temperature dependence of ΔR_H . Below 50 mK, the slope of the resistance starts to flatten presumably as a consequence of the limited thermal coupling of the sample.

DISCUSSION

Ferromagnetic GaMnAs is known to show an increase in resistivity around the Curie temperature, which is assigned to spin disorder scattering of holes by spin fluctuation in the phase transition region.^{17,18} The highest temperature part of the data in Fig. 2 thus reflects the spin ordering process below the Curie temperature of about 45 K, leading to a transient decrease in the resistance. At even lower temperatures, the sheet resistance increases again, which is commonly interpreted as the onset of MIT leading to transport governed by thermally activated hopping. In this case, a behavior $\sim \exp[-(\frac{T}{T_0})^{1/4}]$ is expected assuming variable-range hopping as found by other authors in the temperature range $7 \text{ K} > T > 2 \text{ K}$.^{16,19} The variable-range hopping model, however, fits out data only in a small temperature window between 1.5 and 8 K (see inset of Fig. 2) and clearly fails at lowest temperatures. This proves that it is a different mechanism that leads to a weaker increase of the sheet resistance with decreasing temperature. From the absence of the hopping regime, we conclude that a larger fraction of carriers stay delocalized or weakly localized even down to milli-Kelvin temperatures, where the sheet resistance R_{\square} rises to about 8.5 k Ω , which is close to the Mott critical value of MIT. In MIT theory, the conductivity $\sigma=1/R_{\square}t$ is the important parameter to look at, where t is the sample thickness. Figure 3 convincingly shows that σ exhibits a temperature dependence $\propto T^{1/3}$ below $T=3$ K, spanning a range of 2 orders of magnitude in temperature. Recently, transport measurements above $T=2$ K were interpreted employing weak carrier localization in three-dimensions¹² and the Kondo effect.¹³ The authors predict a temperature dependence $\sigma \propto T^{1/2}$ and $\propto \ln(T)$, respectively, which is not according to our observation. Considering that our data cover a much larger temperature range including temperatures well below 1 K, we want to suggest an alternative interpretation. A temperature dependence of the conductivity $\propto T^{1/3}$ was proposed by 3D scaling theory of Anderson's transition in the presence of strong spin scattering in semiconductors²⁰ and was experimentally found in doped GaAs (Refs. 21–23) and Ge (Ref. 24) semiconductors at low temperatures. According to this theory, close to the MIT, the Fermi liquid theory breaks down and σ is gov-

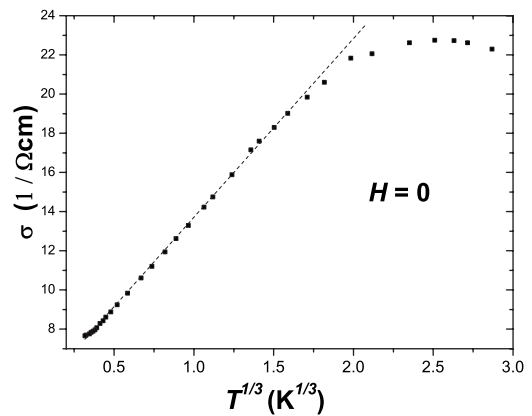


FIG. 3. Conductivity $\sigma=1/R_{\square}t$ plotted versus $T^{1/3}$. $t=150$ nm is the sample thickness. Over 2 orders of magnitude in temperature the conductivity is well described by $\sigma=\sigma_0+\alpha T^{1/3}$, with $\sigma_0=4.5$ ($\Omega \text{ cm}$)⁻¹ and $\alpha=9.11$ ($\Omega \text{ cm K}^{1/3}$)⁻¹ (dashed line).

erned merely by the carrier correlation length ξ and the carrier interaction length $L_T=\sqrt{D\hbar/k_B T}$. Approaching the MIT, ξ diverges, and in the limit $\xi \gg L_T$, the temperature dependence of the conductivity can be written as²¹

$$\sigma = \frac{2}{3} \frac{e^2}{\hbar \xi} + \frac{e^2}{\hbar} \left(\frac{2}{3\pi} \frac{\partial N}{\partial \mu} k_B T \right)^{1/3}. \quad (3)$$

The positive zero temperature conductance $\sigma_0=\sigma(T=0)=4.5$ ($\Omega \text{ cm}$)⁻¹ deduced in Fig. 3 is consistent with the values of the order of ~ 1 ($\Omega \text{ cm}$)⁻¹ found for n -GaAs close to the MIT.^{21–23} Positive values indicate that our sample is still on the metallic side of the MIT as expected. The slope of the conductivity in Fig. 3 enables an estimate of the density of states (DOS) $\partial N/\partial \mu$ at the Fermi level. With $\alpha=9.11$ ($\Omega \text{ cm K}^{1/3}$)⁻¹, we derive $\partial N/\partial \mu \sim 1 \times 10^{44}$ ($1/\text{J m}^3$). For GaMnAs with a higher Mn concentration of 6.25%, first principles calculations predicts a Mn $4p$ and As $4p$ DOSs of about 0.20 and 0.18 ($1/\text{eV atom}$), respectively,²⁵ which correspond to a total DOS of about 1.8×10^{46} ($1/\text{J m}^3$). This is in rather good agreement with our experimental value considering the lower Mn concentration in our samples and the fact that the calculations do not take into account compensation effects due to As_{Ga} antisites and Mn interstitial defects, which are known to reduce the number of holes by up to 80%.¹⁴

For the case of DMSs, the regime close to the MIT is currently under debate and theoretical models that emphasize the disorder in the randomly doped and strongly compensated GaMnAs when carriers become localized have been developed.^{8,9} In contrast to mean-field models, these seem to capture details of the measured magnetic properties such as the slight non-mean-field-like concave shape of the temperature dependence of the magnetization $M(T)$, which some claim to be present even on the metallic side of the MIT.²⁶ It is therefore instructive to look at the temperature dependence of $\Delta R_H/R_{\square}(T)$ shown in Fig. 4, which gives information about changes in the relative magnitude of the AMR. While at high temperatures this ratio increases with decreasing temperature reflecting the increasing spin alignment of the local

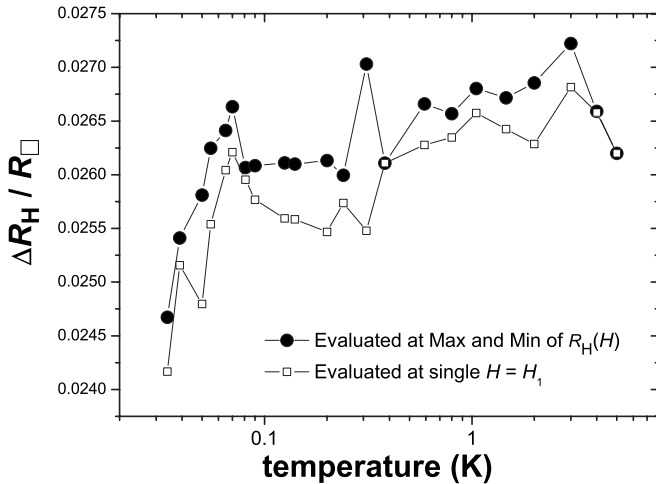


FIG. 4. Temperature dependence of the ratio between the planar Hall-resistance jump ΔR_H and the longitudinal resistance R_\square . For comparison, also an evaluation of ΔR_H at the single field H_1 is shown in open squares. The ratio has a maximum value at around 2 K and decreases by about 6% toward lowest temperatures.

Mn-5/2 moments as shown in earlier works,¹¹ the situation is different in the range below a few Kelvin where the longitudinal resistance R_\square starts to rise. The ratio levels off and seems to exhibit a maximum at a temperature of around 2 ± 1 K. At even lower temperatures below a few Kelvin, where $\sigma \propto T^{1/3}$ holds, a reduction of the relative AMR by $(6 \pm 2)\%$ can be seen. It is conceivable that this decrease is related to the proximity to the MIT and thus the onset of carrier localization. As mentioned in the Introduction, it was recently proposed by theoreticians that, due to inhomogeneous disorder in the randomly doped system, localization of carriers can affect their magnetic properties. Localization of carriers happens preferentially in the vicinity of Mn sites where they are strongly antiferromagnetically coupled to the adjacent Mn spins.²⁶ These localized holes do not play a role in the transport properties of the DMSs such as the AMR but may, to a certain extent, alter the coupling between the local moments and the remaining carriers. A change of the AMR is then expected at lowest temperatures as hinted by our data.

ARONOV-ALTSHULER MODEL APPLIED ON CONDUCTIVITY DATA IN THE LITERATURE

In this section, we want to further support the Aronov-Altshuler model as an alternative interpretation for the transport mechanism in GaMnAs at low temperatures. The theory will, in the following, be applied to existing conductivity data in the literature both on the insulating and metallic sides of the metal-insulator transition. In Figs. 5 and 6, the conductivity of GaMnAs thin films of different Mn concentrations and various annealing treatments are shown according to He *et al.*¹³ and Van Esch *et al.*¹⁹ The nomenclature of the samples corresponds to those of the authors and the main sample parameters are listed in Table I. Assuming $\sigma = \sigma_0 + \alpha T^{1/3}$ as proposed by Aronov-Altshuler, we can fit the conductivity rather well below 6 K, covering the same tempera-

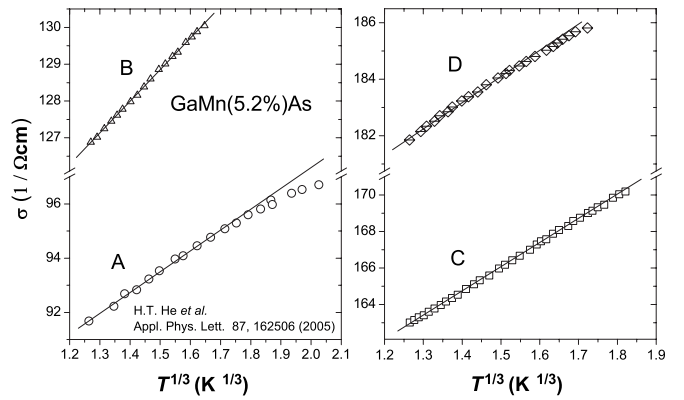


FIG. 5. Conductivity of GaMn(5.2%)As measured by He *et al.* (Ref. 13) for temperatures below 22 K. Samples A, B, C, and D: as grown and annealed at 160, 200, and 260 °C, respectively.

ture range in which Kondo and variable-range hopping models were proposed.^{13,19} The resulting values for σ_0 and α are presented in Table I. For the case of the metallic GaMn(5.2%)As samples A–D (Fig. 5), 2 h annealing at temperatures up to $T=260$ °C increases both σ_0 and α . According to Eq. (3), this is equivalent to an increase of the DOS at the Fermi level and a shift away from the MIT toward the metallic side. This is consistent with the reported reduction of long-range disorder and defect concentrations upon annealing at 260 °C, which leads to an increased hole carrier density and a more effective ferromagnetic coupling between Mn spins.^{3,4} The measurements shown in Fig. 6 include samples with a considerably lower conductivity compared to those of He *et al.* According to Van Esch *et al.*, sample B1 is on the insulator side, B0 and A2 exactly at the MIT, and A1 is metallic. Again, this is reflected in the values for σ_0 : For

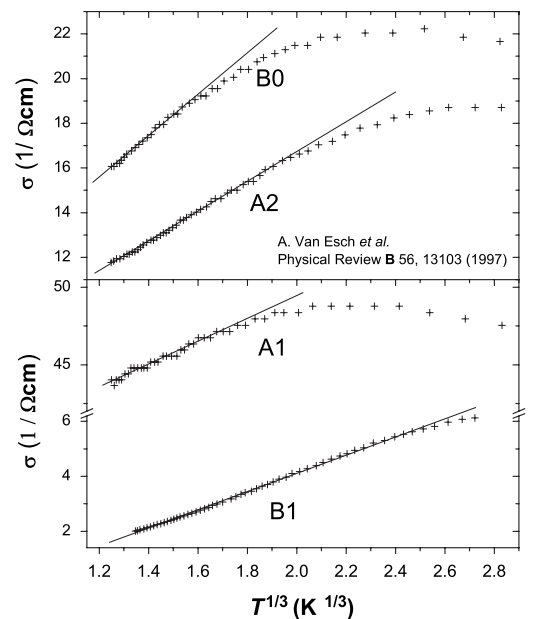


FIG. 6. Conductivity of GaMnAs measured by Van Esch *et al.* (Ref. 19) for temperatures below 22 K. A1 and A2: GaMn(6%)As annealed at 370 and 390 °C, respectively. B0 and B1: GaMn(7%)As as grown and annealed at 370 °C, respectively.

TABLE I. Comparison with those of He *et al.* and Van Esch *et al.*

Sample	Mn (%)	T_a (°C) ^a	σ_0 (Ω cm) ⁻¹	α (Ω cm K ^{1/3}) ⁻¹
A	5.2	As grown	92	0.3
B	5.2	160	116	8.6
C	5.2	200	146	13.1
D	5.2	260	169	10.3
A1	6.0	370	35	7.3
A2	6.0	390	3.3	6.7
B0	7.0	As grown	4.2	9.5
B1	7.0	370	-1.7	2.7

^a T_a denotes the annealing temperature.

B1, the small negative value of -1.7 (Ω cm)⁻¹ suggests the insulating phase but close to the MIT. Like for the case of compensated *n*-GaAs,²¹ it implies that the carrier interaction length L_T determines the conductivity just on the insulating side of the MIT as well. B0 and A2 give small but positive values, indicating metallicity in the proximity of the MIT. Finally, A1 clearly exhibits a metallic character. Furthermore, comparing the as-grown and annealed samples B0 and B1, one observes that α and thus the DOS at the Fermi level are reduced upon annealing at $T=370$ °C. It seems that annealing at higher temperatures has the opposite effect than annealing at $T=260$ °C, as shown for samples A–D. This finding is in agreement with the literature, which reports qualitative changes of the annealing effects above temperatures $T=280$ °C.³ In conclusion, this section shows that despite the limited temperature range of the available data in the literature, the interpretation using the Aronov-Altshuler model leads to reasonable conclusions about the DOS and

metallicity. Changes of measured hole concentrations with different annealing procedures in GaMnAs are well reflected.

V. CONCLUSION

We have studied magnetotransport of epitaxially grown Ga_{0.95}Mn_{0.05}As epilayers with in-plane magnetic easy axis down to temperatures as low as 30 mK. Resistance measurements of our samples show no evidence of strong localization. Instead, a weaker temperature dependence of the conductivity $\propto T^{1/3}$ is observed, which can be well explained by a 3D scaling theory of Anderson's transition in the presence of spin scattering in semiconductors. The results prove that the samples studied are on the metallic side of but very close to the metal-insulator transition. Using the scaling theory, the DOS at the Fermi level was estimated to be $\partial N/\partial\mu \sim 1 \times 10^{44}$ (1/J m³), which is in good agreement with theoretical predictions in the literature. The successful application of the Aronov-Altshuler model on conductivity data by other authors both on the insulating and metallic sides of the metal-insulator transition underlines the potential of this approach. In our measurements of the temperature dependence of the anisotropic magnetoresistance effect, we observe a reduction of the magnitude by (6 ± 2) in the lowest temperature regime, which suggests changes in the interaction between the Mn spins and itinerant carriers in the system. A possible explanation is the observed onset of localization of carriers in the vicinity of local Mn spins.

ACKNOWLEDGMENTS

This research was supported by the DARPA/SPINS program and the Deutsche Forschungsgemeinschaft. We want to thank P. Wigen and A. H. MacDonald for valuable discussions.

*j.honolka@fkf.mpg.de

¹H. Ohno, H. Munekata, T. Penney, S. von Molnár, and L. L. Chang, Phys. Rev. Lett. **68**, 2664 (1992).
²H. Munekata, A. Zaslavski, P. Fumagalli, and R. J. Gambino, Appl. Phys. Lett. **63**, 2929 (1993).
³T. Hayashi, Y. Hashimoto, S. Katsumoto, and Y. Iye, Appl. Phys. Lett. **78**, 1691 (2001).
⁴S. Potashnik, K. Ku, S. Chun, J. Berry, N. Samarth, and P. Schiffer, Appl. Phys. Lett. **79**, 1495 (2001).
⁵T. Dietl, H. Ohno, and F. Matsukura, Phys. Rev. B **63**, 195205 (2001).
⁶J. König, J. Schliemann, T. Jungwirth, and A. H. MacDonald, in *Electronic Structure and Magnetism of Complex Materials*, edited by D. Singh and D. Papaconstantopolos (Springer-Verlag, Berlin, 2001).
⁷M. Paalanen and R. N. Bhatt, Physica B **169**, 153 (1991).
⁸A. Kaminski and S. Das Sarma, Phys. Rev. Lett. **88**, 247202 (2002).
⁹M. Berciu and R. N. Bhatt, Phys. Rev. Lett. **87**, 107203 (2001).
¹⁰S. R. Eric Yang and A. H. MacDonald, Phys. Rev. B **67**, 155202

(2003).

¹¹H. X. Tang, R. K. Kawakami, D. D. Awschalom, and M. L. Roukes, Phys. Rev. Lett. **90**, 107201 (2003).
¹²F. Matsukura, M. Sawicki, T. Dietl, D. Chiba, and H. Ohno, Physica E (Amsterdam) **21**, 1032 (2004).
¹³H. T. He, C. L. Wang, W. Ge, J. N. Wang, X. Dai, and Y. Q. Wang, Appl. Phys. Lett. **87**, 162506 (2005).
¹⁴H. Ohno, J. Magn. Magn. Mater. **200**, 110 (1999).
¹⁵T. Jungwirth, J. Sinova, K. Y. Wang, K. W. Edmonds, R. P. Campion, B. L. Gallagher, C. T. Foxon, Q. Niu, and A. H. MacDonald, Appl. Phys. Lett. **83**, 320 (2003).
¹⁶A. Oiwa, S. Katsumoto, A. Endo, M. Hirasawa, Y. Iye, H. Ohno, F. Matsukura, A. Shen, and Y. Sugawara, Phys. Status Solidi B **205**, 167 (1998).
¹⁷F. Matsukura, H. Ohno, A. Shen, and Y. Sugawara, Phys. Rev. B **57**, R2037 (1998).
¹⁸B. Beschoten, P. A. Crowell, I. Malajovich, D. D. Awschalom, F. Matsukura, A. Shen, and H. Ohno, Phys. Rev. Lett. **83**, 3073 (1999).
¹⁹A. Van Esch, L. Van Bockstal, J. De Boeck, G. Verbanck, A. S.

- van Steenbergen, P. J. Wellmann, B. Grietens, R. Bogaerts, F. Herlach, and G. Borghs, *Phys. Rev. B* **56**, 13103 (1997).
- ²⁰B. L. Altshuler and A. G. Aronov, *JETP Lett.* **37**, 410 (1983).
- ²¹M. C. Maliepaard, M. Pepper, R. Newbury, and G. Hill, *Phys. Rev. Lett.* **61**, 369 (1988).
- ²²D. Romero, S. Liu, H. D. Drew, and K. Ploog, *Phys. Rev. B* **42**, 3179 (1990).
- ²³B. Capoen, G. Biskupsi, and A. Briggs, *J. Phys.: Condens. Matter* **5**, 2545 (1993).
- ²⁴I. Shlimak, M. Kaveh, R. Ussyshkin, V. Ginodman, and L. Resnick, *Phys. Rev. Lett.* **77**, 1103 (1996).
- ²⁵Y.-J. Zhao, W. T. Geng, K. T. Park, and A. J. Freeman, *Phys. Rev. B* **64**, 035207 (2001).
- ²⁶S. Das Sarma, E. H. Hwang, and A. Kaminski, *Phys. Rev. B* **67**, 155201 (2003).